NOTATION

t, time; T, temperature; T_0, ambient temperature; T_m, melting temperature; v, velocity of a point in the liquid medium; U, relative velocity of the bodies; ρ, liquid density, kg/m^3; c, specific heat of the liquid, $J/(m^3 \cdot K)$; λ, thermal conductivity coefficient of the liquid, $W/(m \cdot K)$; μ, dynamic viscosity, $kg/(m \cdot sec)$; $\nu = \mu/\rho$, kinematic viscosity, m^2/sec; r, specific heat of melting, J/kg; h, thickness of the liquid film; a, thermal diffusivity coefficient of the material of the moving body; ℓ, length of the sliding body; b, width of the body.

LITERATURE CITED

1. V. A. Balakin, Friction and Abrasion at High Slipping Velocities [in Russian], Moscow (1980).
2. Wilson, Trans. Amer. Soc. Mech. Eng., J. Tribology, 98, No. 1 (1976).
3. A. K. Stiffler, Trans. Amer. Soc. Mech. Eng., J. Tribology, 106, No. 3, 416-419 (1984).
4. A. Cameron, Theory of Lubrication in Engineering [Russian translation], Moscow (1964).
5. H. S. Carslaw and J. C. Jaeger, Conduction of Heat in Solids, 2nd ed., Clarendon Press, Oxford (1959).

TESTING TWO-TEMPERATURE THERMAL-CONDUCTION THEORY FOR CARBON ROD COMPOSITES

N. A. Vasil'eva, I. V. Goncharov, V. L. Mikov, and V. V. Sazonov

UDC 536.2.01

Measurements have been used to test software for calculating the temperature pattern in a reinforced medium in the two-temperature approximation and for determining model parameters.

Rod composites are widely used, which requires models that adequately reflect heat transfer there; the usual approach is based on homogenizing the composite via effective thermophysical characteristics [1]. The errors are very much dependent on obedience to the conditions for equivalence between a homogeneous medium and the initial heterogeneous one [2], which complicates determining the effective thermophysical parameters. The effective thermal conductivity of a heterogeneous material in general is dependent on time [3].

An alternative description is the two-temperature conduction model, which avoids those difficulties. A representative elementary volume is distinguished, which contains one reinforcing rod in the matrix, and for which one writes averaged conduction equations for each component together with Henry's equation, which relates the heat fluxes between the components q_{ij} to the mean temperatures:

$$q_{ij} = \alpha_c (\hat{T}_i - \hat{T}_j). \tag{1}$$

The correctness of the model has been discussed [4, 5]; it has been used in model treatments [6, 7]. However, its use is hindered by the lack of data on the thermophysical characteristics of the components and also α_c.

Here we present a model for that approach and measurements on the thermal conductivities of carbon rods and matrix; temperature patterns as calculated from the approach are compared with experiment.

Model. We consider a material in which the rods can be divided into two groups: ones in the x–y planes parallel to the surface (denoted by f_{x-y}) and ones parallel to the z axis, f_z; the spaces between the rods are filled with matrix m. Partial homogenization is performed [8] for the f_{x-y} rods and m, and we convert from the multicomponent medium to a two-component one.

Central Special Engineering Research Institute, Khot'kovo. Translated from Inzhenerno-fizicheskii Zhurnal, Vol. 60, No. 6, pp. 968-974, June, 1991. Original article submitted June 26, 1990.

0022-0841/91/6006-0744$12.50

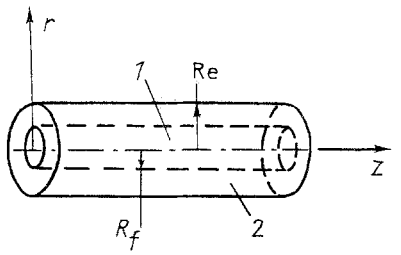

Fig. 1. Representative volume for a composite.

Partial homogenization causes an error in the temperature pattern, but for the carbon-rod materials, that error is slight, since published data [9] indicate that $\lambda_m \approx \lambda_{f\perp}$; then one can distinguish a representative volume consisting of an f_z rod (component 1) and the homogenized medium, component 2 (Fig. 1). The effective radius of the second component is

$$R_e = R_f/\sqrt{\nu_{fz}},$$

in which ν_{fz} is the volume content of the f_z fibers.

The heat propagation in this cylinder with boundary conditions of the first kind is described on the basis of the symmetry by

$$\frac{\partial}{\partial z}\left(\lambda_{zi}\frac{\partial T_i}{\partial z}\right)+\frac{\partial}{\partial r}\left(\lambda_{ri}\frac{\partial T_i}{\partial r}\right)+\frac{\lambda_{ri}}{r}\frac{\partial T_i}{\partial r}=c_i\frac{\partial T_i}{\partial t}, \tag{2}$$

$$T_i(r,\ z,\ 0)=T_0(r,\ z),\ i=1,\ 2, \tag{3}$$

$$-\lambda_{zi}\frac{\partial T_i}{\partial z}\bigg|_{z=0}=\alpha_{g0}(t)\,(T_{g0}-T_i|_{z=0}), \tag{4}$$

$$\lambda_{zi}\frac{\partial T_i}{\partial z}\bigg|_{z=H}=\alpha_{gH}(t)\,(T_{gH}-T_i|_{z=H}), \tag{5}$$

$$T_1(R_f,\ z,\ t)-T_2(R_f,\ z,\ t)=-R_T\lambda_{r1}\frac{\partial T_1}{\partial r}\bigg|_{r=R_f}, \tag{6}$$

$$\lambda_{r1}\frac{\partial T_1}{\partial r}\bigg|_{r=R_f}=\lambda_{r2}\frac{\partial T_2}{\partial r}\bigg|_{r=R_f},\quad \frac{\partial T_2}{\partial r}\bigg|_{r=R_e}=0. \tag{7}$$

We introduce the temperature $\hat{T}_i$ averaged over the cross section of component i:

$$\hat{T}_1(z,\ t)=\frac{2}{R_f^2}\int_0^{R_f}T_1 r dr,\quad \hat{T}_2(z,\ t)=\frac{2}{R_i^2-R_f^2}\int_{R_f}^{R_e}T_2\,r dr.$$

We integrate (2) within each component with weight r and use (7) and (1) to get

$$\frac{\partial}{\partial z}\left(\lambda_{zi}\frac{\partial\hat{T}_i}{\partial z}\right)-c_i\frac{\partial\hat{T}_i}{\partial t}=(-1)^{i+1}\alpha_i(\hat{T}_1-\hat{T}_2),\ i=1,\ 2, \tag{2'}$$

in which $\alpha_1=2\alpha_c/R_f$; $\alpha_2=2\alpha_c R_f/(R_e^2-R_f^2)$.

We write the initial and boundary conditions for (2') by integrating by analogy with (3)-(5):

$$\hat{T}_i(z,\ 0)=\hat{T}_0(z),\ i=1,\ 2, \tag{3'}$$

$$-\lambda_{zi}\frac{\partial\hat{T}_i}{\partial t}\bigg|_{z=0}=\alpha_{g0}(t)\,(T_{g0}-\hat{T}_i|_{z=0}), \tag{4'}$$

$$\lambda_{zi}\frac{\partial\hat{T}_i}{\partial z}\bigg|_{z=H}=\alpha_{gH}(t)\,(T_{gH}-\hat{T}_i|_{z=H}). \tag{5'}$$

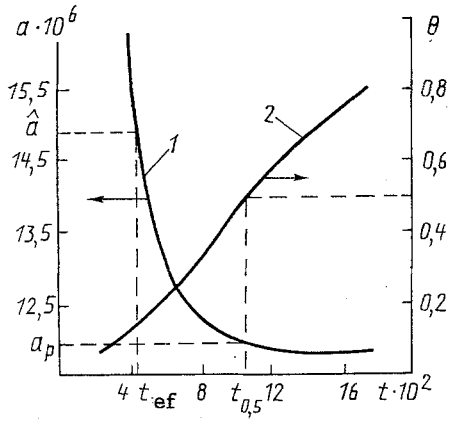

Fig. 2. Relative temperature of reverse surface of specimen θ (2) and thermal diffusivity a_p (1) as time functions; a_p in $m^2 \cdot sec$ and t in sec.

System (2')-(5') describes the temperature pattern on the basis of the nonlinearity in the component characteristics for nonstationary boundary conditions.

These transformations reduce the dimensions from two to one and minimize the number of material characteristics:

$$M_0(\lambda_{zi}, \lambda_{ri}, c_i, i=1, 2; R_T) \rightarrow M_2(\lambda_{zi}, c_i, i=1, 2; \alpha_c).$$

The heat-transfer coefficient α_c between rods and matrix is an integral characteristic, and it is evident that $\alpha_c = f(\lambda_{ri}, i = 1, 2; R_T)$.

Finite differences [10] are used to solve (2')-(5'); the inexplicit difference algorithm was used with a uniform net and step h in the coordinate and step Δt in time as

$$c(\hat{T}_i^s)(\hat{T}_{ij}^{s+1} - \hat{T}_{ij}^n) = \frac{\Delta t}{h^2}[\lambda_{zi}^{j+1}(\hat{T}_i^s)(\hat{T}_{ij+1}^{s+1} - \hat{T}_{ij}^{s+1}) -$$

$$- \lambda_{zi}^{j}(\hat{T}_i^s)(\hat{T}_{ij}^{s+1} - \hat{T}_{ij-1}^{s+1})] - \Delta t \alpha_i(\hat{T}_i^s)(\hat{T}_{1j}^s - \hat{T}_{2j}^s)(-1)^{i+1}, \quad i = 1, 2,$$

in which

$$\lambda_{zi}^{j}(\hat{T}_i^s) = \lambda_{zi}^{j}\left(\frac{\hat{T}_{ij-1}^s + \hat{T}_{ij}^s}{2}\right),$$

with s the number of the iteration, j the number of the coordinate step, and n the number of the time step.

The system is solved iteratively, with the check on the accuracy from

$$\max_j |\hat{T}_{ij}^{s+1} - \hat{T}_{ij}^s| / \max_j |\hat{T}_{ij}^{s+1}| \leqslant \varepsilon,$$

in which ε is the set accuracy.

That algorithm has been implemented in the SOSTK Fortran IV program for the ES computers; the run time was on average 5 min. Tests against the exact analytic solution [5] indicate an error of not more than 1%.

A typical composite as described below was used to evaluate the performance.

The composite consisted of carbon rods immersed in a carbon sinter (matrix); each rod consisted of several thousand carbon fibers also impregnated with the sinter. To a first approximation, the rods may be considered as homogeneous. In the x–y plane, there are three rows of $f_{x\text{-}y}$ rods displaced by 60° one relative to another, together with one row of rods parallel to the z axis, f_z. The rod diameter $2R_f$ = 1.2 mm, calculated geometrical value ν_{fz} = 0.17.

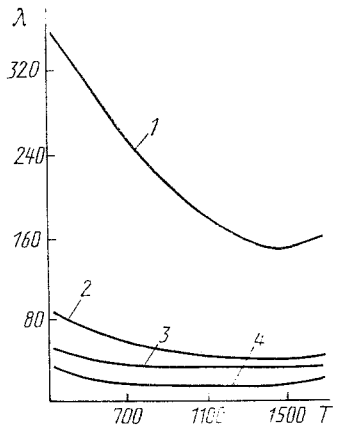

Fig. 3. Temperature dependence of thermal conductivities: 1) λ_{z1}; 2) $\hat{\lambda}$; 3) λ_p; 4) λ_{z2}. λ, W/(m·K); T, K.

Parameter Determination. The temperature pattern may be determined from the set of characteristics $M_2(\lambda_{z1}, \lambda_{z2}, c_1, c_2, \alpha_c)$.

The specific heats of the fibers and matrix (sinter) may be taken as the same as that of graphite [11] because the specific heat is governed by the composition. The component densities were calculated from

$$\rho_2 = \left\{\sum_{i=1}^{3} \rho_f \nu_{fi} + \rho_m \left(1 - \nu_{fz} - \sum_{i=1}^{3} \nu_{fi} - P\right)\right\} / (1 - \nu_{fz}), \quad \rho_1 = \rho_f.$$

Here ν_{fi} is the volume proportion of the rod group f_{x-y}, i = 1, 2, 3, which can be transformed to

$$\rho_2 = \rho_f + \left[\Delta\rho \left(1 - \frac{\sum_{i=1}^{3} \nu_{fi}}{1 - \nu_{fz}}\right) - \rho_m \frac{P}{1 - \nu_{fz}}\right], \tag{8}$$

in which $\Delta\rho = \rho_m - \rho_f$: estimates show that the terms in the square brackets are small in magnitude and are opposite in sign, so one can write $\rho_2 \simeq \rho_f$ with an error of not more than 5%.

The component conductances were determined with a Sinku-Riko commercial pulse system, which employs Parker's method [12]. Aspects of using such a technique with composites have repeatedly been discussed [13, 14], but a realistic method of processing the data has been given only in [15]. Disadvantages are the need to use several specimens differing in thickness and the lack of a rigorous theoretical basis. We employed a method based on solving the inverse coefficient problem (SONDI), which used the pulse results to determine λ_{z1}, λ_{z2}, and α_c [16].

The SONDI treatment was evaluated on a test case for steel reinforced with copper wire (diameter ~1 mm) along the heat treatment direction. For a specimen of standard diameter ~10 mm, we were able to place seven reinforcing rods (ν_{fz} = 0.07). The test data gave thermal conductivities of 340 and 39.9 W/m·K for copper and steel correspondingly at 600 K, which differ from reference data by not more than 10%. Then the effective thermal conductivity is

$$\hat{\lambda} = \lambda_{z1}\nu_{fz} + \lambda_{z2}(1 - \nu_{fz}) \tag{9}$$

which is used to determine the effective thermal diffusivity

$$\hat{a} = \hat{\lambda} / \hat{c},$$

in which $\hat{c} = c_1\nu_{fz} + c_2(1 - \nu_{fz})$.

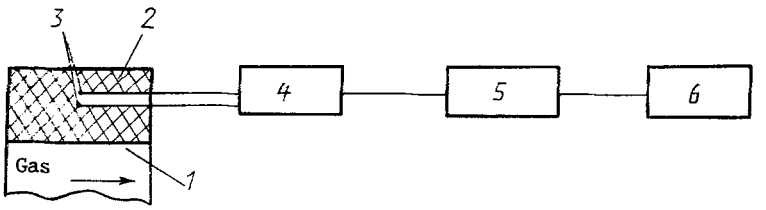

Fig. 4. Experiment scheme.

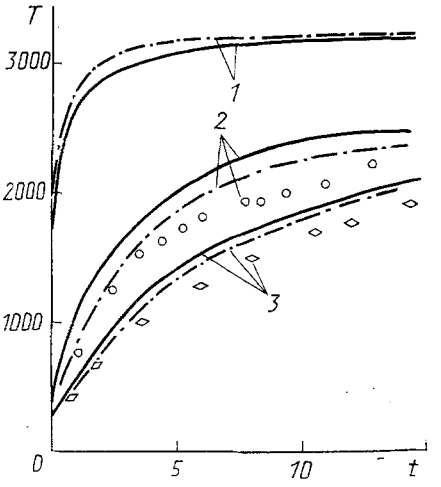

Fig. 5. Comparison of measurements with numerical data for depths of 1) z = 0; 2) 5.2; 3) 8.5; points from experiment, dot–dashed curves from two-temperature model, solid lines from one-temperature model.

Figure 2 shows the relative temperature at the back surface θ as a function of time and the corresponding variation in the thermal diffusivity $a_p(t)$ calculated by Parker's method [12]; the exact value of the diffusivity $\hat{\alpha}$ is much higher than the $\alpha_p(t_{0,5})$ used in practice.

We then performed tests on the composite (diameter ~10 mm, thickness ~2-3 mm), where Fig. 3 shows $\lambda_{z1}(T)$, $\lambda_{z2}(T)$ derived from the SONDI treatment, as well as the $\lambda(T)$ from (9) and $\lambda_p = \alpha_p(t_{0,5})\hat{c}$, the effective thermal conductivity of the composite as determined as in [12]. Here we obtained a result analogous to that discussed above: $\hat{\lambda} > \lambda_p(t_{0,5})$ throughout the temperature range.

There are systematic measurement errors due to inhomogeneity in the laser pulse distribution and a size of ~4 mm for the pyrometer spot, and also uncertainty over ρ_2, which reduced the accuracy considerably: $\delta\lambda_{z1} \leq 10\%$, $\delta\lambda_{z2} \leq 12\%$, $\delta\alpha_c \leq 18\%$.

Experimental Results. To evaluate the model, we tested it with a high-enthalpy gas flow (Fig. 4) used at the surface of a cylindrical flow system (1) composed of the composite (2). At various distances from that surface, there were thermocouples (3) of VR5/20 type having yttrium oxide insulation. The thermocouple readings were processed by the apparatus 4, telemetry system 5, and computer 6. The over-all measurement error did not exceed 12%.

The temperature pattern was simulated in two ways: by solving the one-temperature case for nonlinear thermal conductivity with effective values $\lambda_p \to T_p$ and via the SOSTK treatment for the approach to T_D by the use of a set of derived model parameters: $\{\lambda_{z1}, \lambda_{z2}, \alpha_c\}$ (with geometrical extrapolation for the Fig. 3 data to 3200 K). Figure 5 compares the experimental T_e with the calculated T_p and tT_D for various depths; $T_D(z, t)$ was much closer to the measured values, error not more than 10%, which is within the experimental error. The largest differences between the calculated values occurred at the boundary. Proper correction for the working conditions (oblation, cylindrical geometry, and so on) reduces the differences between the observed and theoretical results.

Conclusions. This software simulates heat transfer in reinforced media and consists of the SONDI program, which processes test data, and the SOSTK program, which solves the coupled nonlinear thermal-conduction equations.

NOTATION. T_i and $\hat{T}_i$, temperature and mean temperature over the cross section for component i; q_{ij} heat flux density from component i to component j; c_i, ρ_i, λ_{ri}, λ_{zi} specific heat, density, and radial and axial thermal conductivities correspondingly; α_c and R_T, heat-transfer coefficient and contact thermal resistance between components; α_{g0} (α_{gH}), heat-transfer coefficient between gas and composite; T_{g0} (T_{gH}), gas temperature; R_f rod radius.

LITERATURE CITED

1. G. N. Dul'nev and Yu. P. Zarichnyak, Thermal Conductivities of Mixtures and Composites [in Russian], Leningrad (1974).
2. L. A. Kozdoba, Proceedings of the Seventh All-Union Conference on Heat and Mass Transfer [in Russian], Vol. 7, Minsk (1984), pp. 34-39.
3. G. C. J. Bart, C. J. Hoogendoorn, and P. B. J. Schaareman, Warme- und Stoffubertragung, 20, No. 4, 269-272 (1986).
4. L. P. Khoroshun and Yu. A. Ivanov. Prikl. Mekh., 21, No. 11, 43-50 (1985).
5. I. V. Goncharov and V. L. Mikov, Inzh.-fiz. Zh., 58, No. 2, 311-316 (1990).
6. V. V. Vorobei, Yu. A. Ivanov, and L. P. Khoroshun, Prikl. Mekh., 22, No. 10, 86-91 (1986).
7. I. V. Goncharov and V. L. Mikov, "The temperature pattern in a reinforced composite for boundary conditions of the second kind," deposited at VIMI January 19, 1989, No. D07661.
8. D. L. Balageas, HT-HP, 16, No. 2, 199-208 (1984).
9. J. Jortner, Winter Annual Meeting of the American Society of Mechanical Engineers, Arizona (1982), pp. 19-27.
10. R. Richtmayer and C. Morton, Difference Methods of Solving Boundary-Value Problems [Russian translation], Moscow (1972).
11. C. G. Goetzel, HT-HP, 12, No. 1, 11-22 (1980).
12. W. J. Parker, R. J. Jenkins, and C. P. Butler, J. Appl. Phys., 32, No. 9, 1679-1683 (1961).
13. R. L. Shoemaker, HT-HP, 18, No. 6, 645-654 (1986).
14. R. Taylor, J. Jortner, and H. Groot, Carbon, 23, No. 2, 215-222 (1985).
15. R. M. Pujola and D. L. Balageas, HT-HP, 17, No. 6, 623-632 (1985).
16. I. V. Goncharov and V. L. Mikov, Inzh.-fiz. Zh., 58, No. 3, 493-495 (1990).

SPECIFIC HEAT AND THERMODYNAMIC CHARACTERISTICS OF THE SYSTEM Bi—Sr—Ca—Mg—Cu—O IN THE TEMPERATURE RANGE 4.2-300 K

E. M. Gololobov, B. V. Novysh,
N. A. Prytkova, Zh. M. Tomilo,
N. M. Shimanskaya, Ya. A. Abeliov,
G. V. Maiornikova, and A. B. Yagina

UDC 537.312.62

Results are presented from an experimental study of specific heat of the superconductive metal oxide system Bi—Sr—Ca—Mg—Cu—O over the temperature range 4.2-300 K. Temperature-dependent components of entropy and enthalpy are calculated. A correlation is made between T_c and standard entropy and enthalpy values for high temperature superconductors of various classes.

There is a current trend toward deeper study of high temperature superconductor (HTSC) materials in order to accumulate information on this phenomenon, the physical nature of which is still unclear. In this respect the thermodynamic characteristics and their standard values are important for constructing phase diagrams in various coordinate systems, determining the character of phase transitions, etc. [1-3]. Such data are very lacking for HTSC materials [4-6].

Translated from Inzhenerno-fizicheskii Zhurnal, Vol. 60, No. 6, pp. 974-979, June, 1991. Original article submitted July 12, 1990.

0022-0841/91/6006-0749$12.50